euspen's 24th International Conference & Exhibition, Dublin, IE, June 2024
www.euspen.eu

Modelling and analysis of cutting forces in ultraprecision diamond turning of freeform surfaces and their assessment

Shangkuan Liu[1], Kai Cheng[1] and Joe Armstrong[2]

[1]*Department of Mechanical and Aerospace Engineering, Brunel University London, Uxbridge, London, UK*
[2]*Polytec GmbH, Polytec-Platz 1-7, 76337 Waldbronn, Germany*

Emails: Shangkuan.Liu@brunel.ac.uk; Kai.Cheng@brunel.ac.uk; j.armstrong@polytec.de

Abstract

In the realm of ultraprecision manufacturing freeform surfaced optics and devices, the ultraprecision diamond turning process holds significant prominence. While cutting force, a pivotal physical parameter in the machining process, has received substantial attention in R&D and machining practices, scant emphasis has been placed on elucidating the nuances of cutting forces and the associated cutting dynamics in ultraprecision diamond turning of freeform surfaces particularly through fast and/or slow tool servo (FTS / STS) modes. In this paper, theoretical analysis on the cutting force and its modelling are presented in the ultraprecision diamond turning of freeform surfaces, particularly considering constant variations of cutting forces along the freeform surface curvature and the increasingly stringent requirement on high precision optical surface finishing. The cutting forces modelling is based on integration of Akins model with the influence of shear angles varying constantly on the freeform surface conduction. Based on the toolpath data of the cutting process at the freeform surface, the depth-of-cut (DoC) of the surface, curvature variations, and shear angle variations throughout the process are meticulously analysed. Subsequently, a cutting force model is developed to discern the nuances of the cutting motion by analysing the cutting toolpath, and then consequently enabling the prediction of cutting forces variation during orthogonal cutting motion with a round-edged diamond cutting tool. Finally, an integrated approach for examining the correlation between cutting forces and the analysis of surface texture and texture aspect ratio should be developed and further investigated, particularly on the functionality of a freeform surface and its generation in ultraprecision machining.

Keywords: Cutting force modelling; ultraprecision diamond turning; freeform surfaces; micro cutting mechanics; surface texture aspect ratio; freeform optics.

1. Introduction

The fast-/slow-tool servo (F-/STS) diamond turning process, known for its high determinism, has seen significant success in producing micro-structured functional freeform surfaces and been widely introduced into the area with high requirement of high customization and nanometre's level surface roughness in recent years. The fundamental kinematic feature in cutting motion between the fast and slow tool servo systems exhibits similarities: the workpiece follows the spindle in rotational movement, while the diamond tool tip cutter moves uniformly along the x-axis at the centre height of the spindle and precisely follow the designed micro-structure and moved in the z-direction. Eventually the desired freeform surface can be produced with high quality promised. The technique ensures the surface roughness quality of the product surface, achieving as low as 1-10 nm.

In the last three decades, there is a large amount of research and efforts in diamond turning machine development, in ultraprecision cutting, single-point diamond turning (SPDT) stands out as the primary method for achieving surface roughness at the nanometer level [1]. In SPDT machining process, the cutting tool material consists of a single-crystal diamond with a small diameter cutting edge. This nanoscale cutting edge facilitates the production of smooth surfaces with minimal damage to the top surface [2]. Apart from traditional slow tool servo cutting technology, fast tool servo cutting is employed to achieve high accuracy on complex non-spherical surfaces and microstructures [3]. Furthermore, due to the rapid development and widespread application of freeform surfaces, optimizing freeform surface toolpath generation has become increasingly vital in the state-of-the-art ultra-precision machining field [4][5]. In the Single Point Diamond Turning (SPDT) process, research has been conducted to explore the capabilities in different materials [6][7] and shapes [8]. In addition, some integrated research explores such as Macro-micro dual -drive technology, contributing to the advancement of both ultra-precision systems and macro–micro dual-drive technology [9].

The cutting force holds paramount significance in the single-point diamond turning machining process as it reflects the direct interaction between the cutter and the workpiece. Leveraging the wealth of information derived from the toolpath data, which is intricately linked to the designed freeform surface, cutting force modelling emerges as a highly promising approach for ensuring the quality control of the designed surface. Over the past decade, extensive research has been conducted on cutting force in single-point diamond turning machining processes. This research encompasses areas such as cutting force prediction, analysis of cutter kinematic motion, including cutting force tracking and prediction [10], cutting force control for improved surface results, and the investigation of the relationship between chip loads and cutting force fluctuations [11], etc. The anticipation of required cutting forces in advance serves as the foundational element for linking resulting surface quality to the cutting process."

In the SPDT machining process, the fabrication of freeform surfaces presents a notable challenge due to the continuous changes in surface curvature. These dynamic alterations correspondingly lead to variations in cutting angles during the machining process. The inherent changes in curvature directly influence both the cutting angles and the depth of cutting (DoC) of the cutter, consequently affecting the cutting forces throughout the machining operation. Through an analysis of the toolpath file and the prediction of variations across the entire cutting loop, it becomes possible to examine the positional relationships among each cutter location point. This analysis aids in identifying problematic or challenging areas on the designed surface. From an industrial perspective, the utilization of toolpath analysis serves a dual purpose. Firstly, it provides the means to retrospectively trace the cutting process, enabling the identification of factors that may have contributed to the production of faulty parts. Secondly, this retrospective analysis serves as a valuable tool for preventing similar challenges in subsequent production cycles, contributing to enhanced efficiency and product quality.

This paper is focused on the cutting force variances with the height position changes in the z-axis, which leads to the varies DoC and angles of kinematics. It aims to investigate the relationship between the designed freeform surface curvature changes, 3D surfaces parameters analysis of the surface, and the resulting cutting force to enhance the precision and quality of microstructured surfaces.

2. Methods

2.1. STS process toolpath interpretation and analysis

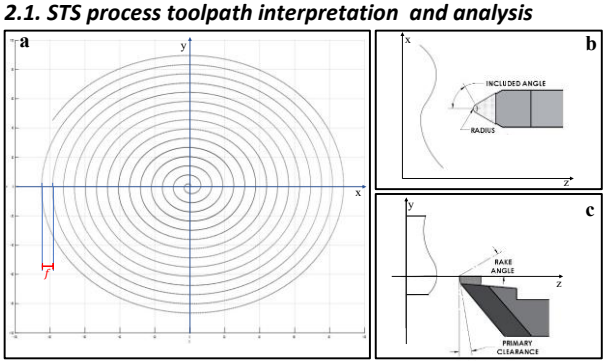

Figure 1. Schematic of cutting kinematics of diamond turning machining. a) the toolpath of the surface in the XOY plane; b) the tooltips and surface relationship at the top view and c) the lateral view of the cutting process.

As depicted in Fig.1(a), the trajectory of the machine tool in STS mode can be conceptualized as the Archimedes spiral pattern motion of the cutter within the $O-X\theta Z$ cylindrical coordinate system. In this system, the XOY plane is aligned parallel to the spindle surface. On this plane, the cutter's movement follows a linear motion with uniform speed along the X-axis direction (either from the center to the edge or vice versa). This motion is coordinated with the rotational movement of the spindle in the C-axis. As a result, an Archimedean spiral pattern is generated, with a predetermined distance between each point and a specified feed rate. These parameters significantly influence the number of points in each circle and the number of circles the cutter needs to traverse, which, in turn, has a substantial impact on the resulting quality and processing time of the machine. The specific values of these parameters are generally dependent on the tool radius.

The YOZ plane runs parallel to the plane defined by the cutting edge of the tool, while the XOZ plane illustrates the correlation between the tool radius and the movement along the x-direction. Both planes collectively portray the motion of the cutter along the Z-axis direction. Understanding and optimizing these trajectories are crucial for achieving precise and efficient machining, considering the interplay between tool geometry and the chosen toolpath strategy.

2.2. Cutting force and shear force

The cutting force model developed in this study is grounded in Atkins' model [12]. Simultaneously, we consider the direction of the cutting force and the practical DoC. In instances where surface work plays a substantial role in steady deformation, several internal works are identified: (i) plasticity along the shear plane; (ii) friction along the underside of the chip at the tool interface; and (iii) formation of a new cut surface [12]. All these work components are externally provided by the FC component of the tool force moving along the machined surface's toolpath file.

2.3. Cutting force model in STS process

To estimate the practical cutting force based on the toolpath data, the practical shear direction needs to be first been calculated below:

$$\phi = \frac{\pi}{4} - \frac{\beta - \alpha}{2} \tag{1}$$

In this scenario, where β represents the friction angle along the rake face, and α is the tool rake angle. Simultaneously, with the cutter transitioning from the (i-1)-th to the i-th point, the relative distance between these two location points can be calculated using the following function [13]:

$$d = \sqrt{f^2 + (z1 - z2)^2} \tag{2}$$

where f represents the feed rate along the X-axis of the cutting process, and z1 and z2 are the positional data along the Z-axis. The included angle α_o between these two points can be expressed by

$$\alpha_0 = \arctan\left(\frac{z1 - z2}{f}\right) \tag{3}$$

The coordinates of the intersection point A (Xa, Za) between the cutter edge at the previous (i-1)-th point and the current i-th point can be calculated by

$$\begin{cases} x_a = -\frac{1}{2}f - \sqrt{r^2 - \left(\frac{d}{2}\right)^2}\sin(\alpha_0) \\ z_a = \frac{1}{2}(z1 + z2) - \sqrt{r^2 - \left(\frac{d}{2}\right)^2}\cos(\alpha_0) \end{cases} \tag{4}$$

The coordinates of the intersection points B (Xb, Zb) and C (Xc, Zc), corresponding to the cutter edge at the preceding (i-1)-th point and the current i-th point, with the uncut surface, can be calculated by

$$\begin{cases} x_b = \sqrt{r^2 - (z1 - h_0)^2} - f \\ z_b = z_c = h_0 \end{cases} \tag{5}$$

Where h_0 is the height of the uncut surface in the toolpath data. And the relative angle between the i-th point to point A, B, and C respectively can be obtained as

$$\begin{cases} \theta_a = \arcsin\left(\frac{x_a}{r}\right) \\ \theta_b = \arctan\left(\frac{x_b}{z2 - h_0}\right) \\ \theta_c = \arcsin\left(\frac{x_c}{r}\right) \end{cases} \tag{6}$$

Accordingly, the practical DoC can be calculated by using the equations (7) below.

$$\begin{cases} DoC = \frac{1 - \cos(\alpha_0 + \theta_i + \alpha_1)}{\cos(\alpha_0 + \theta_i)}, \text{where } \theta_a \le \theta_i < \theta_b \\ DoC = r\cos(\alpha_0) - \frac{z2 - h0}{\cos(\theta_i)}\cos(\alpha_0), \text{where } \theta_b \le \theta_i < \theta_c \end{cases} \tag{7}$$

With the help of Atkins' model, the overall main cutting force can be obtained as follows:

$$F_cV = (\tau_y\gamma)(t_0wV) + [F_c \sec(\beta - \alpha)\sin\beta]\frac{V\sin\phi}{\cos(\phi - \alpha)} + RwV \quad (8)$$

where V is the cutting velocity, F_c is the horizontal component of the cutting force, τ_y is the (rigid-plastic) shear yield stress, γ is the shear strain along the shear plane, given by $\gamma = cot\varphi + \tan(\varphi - \alpha) = cos\alpha/\cos(\varphi - \alpha)sin\varphi$; t0 is the uncut chip thickness, w is the width of the orthogonal cut, φ is the orientation of the shear plane and R is the specific work of surface formation (fracture toughness). The constant parameters using for calculation have been listed in the Table 1.

Table 1 Constant parameters using in the calculation

Parameters	Definition	value
Vr	(r/s) Spindle rotation speed	3000
τ_y	(Mpa) Shear yield stress	55.2
μ	The coefficient of friction	0.583
r	(mm) Tool radius	0.35
D	(mm) Objective surface diameter	78
α	(mm) Tool rake angle	0

3. Results and discussion

3.1 Experiment setup

Fig. 2(a) illustrates the cutting motion in the process, highlighting the mirror surface machining procedure that employs a carrier disk. As depicted in Figure 2(b), the diameter of the disk is 290mm, and the capacity of the carrier disk allows the machine to work on six mirrors simultaneously. The distribution of mirrors is symmetrical from left to right, with two mirrors allocated on the top and bottom, and one each on the left and right. The cutter works concurrently on six mirrors within the container, continuously transitioning between kinematic motion and movement toward the next surface.

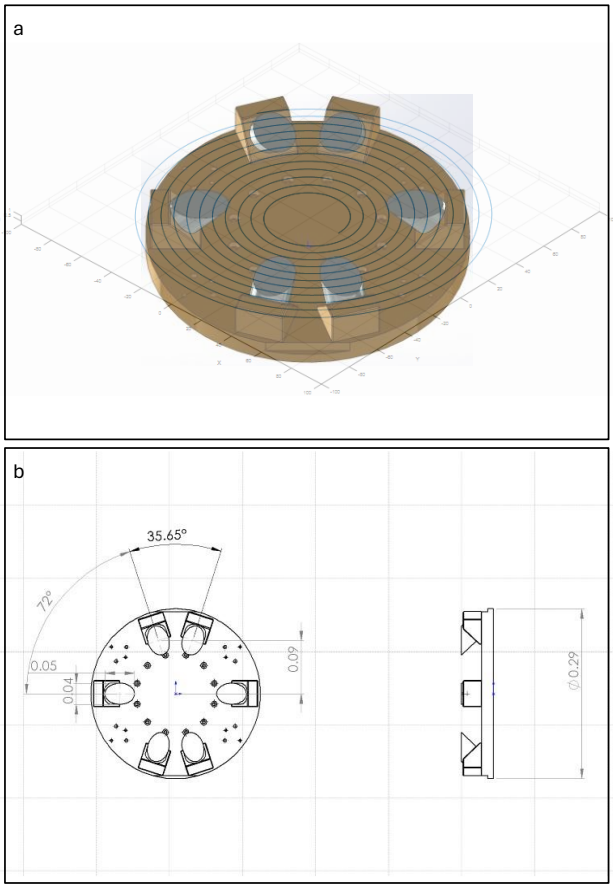

Figure 2. a) Cutting motion in the process and mirror surface machining procedure with a carrier disk. b) Parameters and spread of the workpieces on the carrier disc

3.2 Modelling results and discussion

The estimated primary cutting force is depicted in Fig. 3. The selected estimated cutting force corresponds to the tool movement along the X-axis, spanning from 18.76 cm to 18.9 cm (utilizing 206,460 cutter location points). The illustration demonstrates a commendable accordance, perfectly reflecting the variations in cutter kinematics as it moves between each surface without any cutting progress.

To provide a more detailed insight into the characteristics of cutting force changes during the cutting progress, a specific loop was selected when the cutter's location on the X-axis ranged between 18.86cm and 18.87cm, with a focus on material removal from the surface. A clear periodicity is observed in this motion, with the estimated minimum cutting force occurring when the cutter is positioned at 18.8642 along the X-axis. At this point, the cutting force is recorded as 0.0120778 N.

As illustrated in Fig. 4, as the practical shear angle decreases, the rising trend of the cutting force becomes negative, eventually showing a decline. As the cutter moves into the material removal area, the changes in shear angle become more frequent but remain subtle. Notably, the cutting force exhibits a similar trend of change. These findings indicate that the developed model adeptly captures the cutter's location based on the toolpath data and process parameters associated with material removal in the diamond turning machining process.

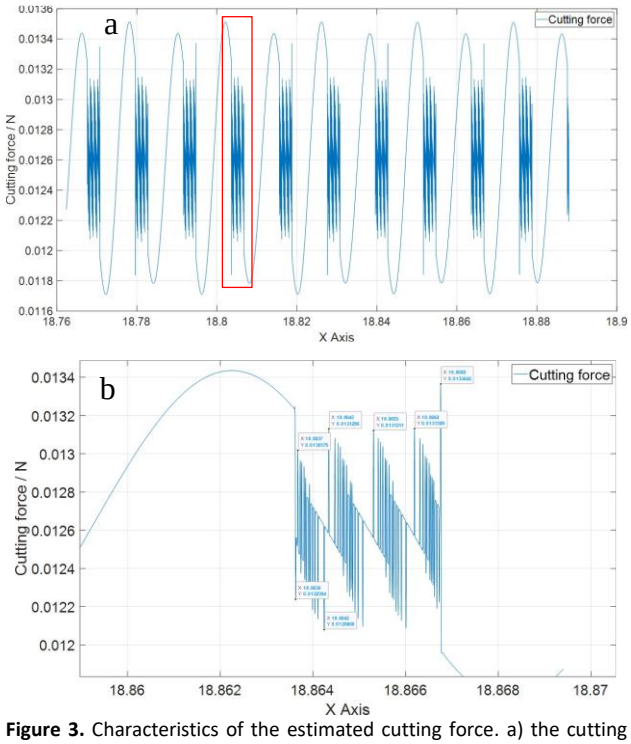

Figure 3. Characteristics of the estimated cutting force. a) the cutting force from 18.76 cm to 18.9 cm, b) the cutting force plot only focus on the red frame part (from 18.86cm to 18.87cm).

Figure 5 illustrates a 3D surface topography obtained after SPDT machining process. Stitched profilometer image of 3 mm area from a curved surface area with form removed using software showing machine tool travel across the surface with numerical

texture 2D and 3D areal parameters. 2D profile lines are in line with the tool path direction.

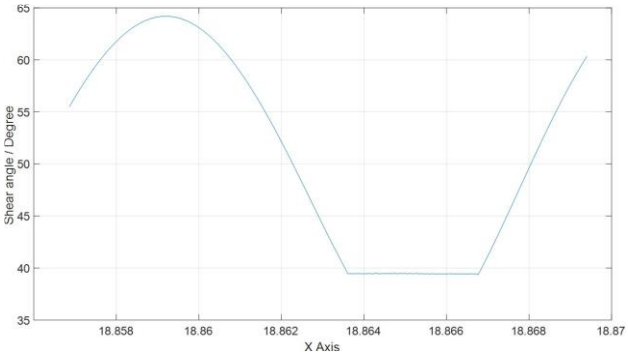

Figure 4. The practical shear angle.

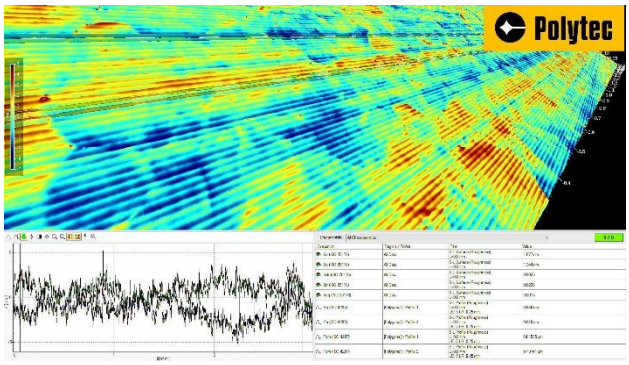

Figure 5. The 3D surface topography assessment result of machined surface by using white light interferometers.

4. Conclusions

In this research, we developed a cutting force model that considers the influence of cutting angles and the corresponding DoC, utilizing machine toolpath data. To achieve this, we extracted and thoroughly investigated the machine toolpath. Calculated the practical shear angle, relative distances between each cutter location point, and the practical Depth of Cut. These parameters were then incorporated into the final cutting force calculations. In future work, the current model lacks control interfaces, making it unable to directly import toolpaths. Secondly, the model currently lacks comparative data for expanded parameters such as residual height and the relationship between cutter radius and cutting force. Lastly, ongoing efforts involve the comparison of the model's predictions with real-world data. The surface of toolpath file has been machined, and observations have been conducted using a white light interferometer. The current phase involves the organization and analysis of the collected data.

Nomenclature

STS	Slow-tool servo diamond turning process
SPDT	Single-point diamond turning machining process
DoC	Depth of cutting
ϕ	Practical shear direction
β	Friction angle along the rake face
α	Tool rake angle
d	the relative distance between two continues location points
f	Feed rate of the cutter in the machine process
z1 z2	the two positional data of the cutter along the Z-axis
α_0	The practical included angle of the cutter in the process
x_a, x_b, x_c	The location data in the X-axis at the intersection points between the cutter edge at the (i-1)th point and the (i)th point.
z_a, z_b, z_c	The location data in the Z-axis at the (i-1)th and (i)th intersection points between the cutter edge and the uncut surface.
h_0	Height of the uncut surface in the toolpath data
$\theta_a, \theta_b, \theta_c$	Relative angle between the (i) point to point A, B, and C
F_c	Cutting force
V	Cutting velocity
τ_y	Shear yield stress
t_0	Uncut chip thickness
w	Width of the orthogonal cut
γ	Shear strain along the shear plane
φ	Orientation of the shear plane
R	Fracture toughness

References

[1] Yip, W. S., To, S., & Zhou, H. (2022). Current status, challenges and opportunities of sustainable ultra-precision manufacturing. Journal of Intelligent Manufacturing, 1-13.

[2] Yip, W. S., Yan, H. E., Zhang, B., & To, S. (2024). The state-of-art review of ultraprecision machining using text mining: Identification of main themes and recommendations for the future direction. Wiley Interdisciplinary Reviews: Data Mining and Knowledge Discovery, 14(1), e1517.

[3] Gong, Z., Huo, D., Niu, Z., Chen, W., & Cheng, K. (2022). A novel long-stroke fast tool servo system with counterbalance and its application to the ultra-precision machining of microstructured surfaces. Mechanical Systems and Signal Processing, 173, 109063.

[4] Cheng, K. and Huo, D. (Editors), Micro Cutting: Fundamentals and Applications, John Wiley & Sons, Chichester, October 2013.

[5] He, S., Xuan, J., Du, W., Xia, Q., Xiong, S., Zhang, L. & Shi, T. (2020). Spiral tool path generation method in a NURBS parameter space for the ultra-precision diamond turning of freeform surfaces. Journal of Manufacturing Processes, 60, 340-355.

[6] Mukaida, M. & Yan, J. (2017). Ductile machining of single-crystal silicon for microlens arrays by ultraprecision diamond turning using a slow tool servo. International Journal of Machine Tools and Manufacture, 115, 2-14.

[7] Sawangsri, W. & Cheng, K. (2016). An innovative approach to cutting force modelling in diamond turning and its correlation analysis with tool wear, Proceedings of the IMechE, Part B: Journal of Engineering Manufacture, 230(3), 405-415.

[8] To, S., Zhu, Z., & Wang, H. (2016). Virtual spindle based tool servo diamond turning of discontinuously structured microoptics arrays. CIRP Annals, 65(1), 475-478.

[9] Yang, M., Gui, H., Zhang, C., Zhao, S., Han, F., Dang, M., & Zhang, B. (2023). Recent development for ultra-precision macro–micro dual-drive system: A review. Machines, 11(1), 96.

[10] Chen, Y. L., Cai, Y., Tohyama, K., Shimizu, Y., Ito, S., & Gao, W. (2017). Auto-tracking single point diamond cutting on non-planar brittle material substrates by a high-rigidity force controlled fast tool servo. Precision Engineering, 49, 253-261.

[11] Zhou, X., Wang, R., & Liu, Q. (2017). Study on suppressing cutting force fluctuations based on chip loads for turning optical freeform surfaces. The International Journal of Advanced Manufacturing Technology, 90, 2037-2046.

[12] Atkins, A. G. (2003). Modelling metal cutting using modern ductile fracture mechanics: quantitative explanations for some longstanding problems. International journal of mechanical sciences, 45(2), 373-396.

[13] Zhu, Z., To, S., Zhu, W. L., Huang, P., & Zhou, X. (2019). Cutting forces in fast-/slow tool servo diamond turning of micro-structured surfaces. International Journal of Machine Tools and Manufacture, 136, 62-75.